

Version of December 2, 2024

## The Remarkable Be Star HD110432 (BZ Cru)

Myron A. Smith,

*Catholic University of America,  
3700 San Martin Dr., Baltimore, MD 21218;  
msmith@stsci.edu*

and

Luis Balona<sup>1</sup>

*South African Astronomical Observatory,  
P. O. Box 9, Observatory 7935, South Africa;  
lab@sao.ac.za*

### ABSTRACT

HD 110432 has gained astronomical attention because it is a hard, variable X-ray source and also because its optical spectrum is affected by an extensive Be disk. From time-serial echelle data obtained over two weeks during 2005 January and February, we find several remarkable characteristics in the star's optical spectrum. The line profiles show rapid variations on some nights which can most likely be attributed to irregularly occurring and short-lived *migrating subfeatures*. Such features have only been observed to date in  $\gamma$  Cas and AB Dor, two stars for which it is believed magnetic fields force circumstellar clouds to corotate over the star's surface. The star's optical spectrum also exhibits a number of mainly Fe II and He I emission features with profiles typical of an optically thin circumstellar disk viewed edge-on. Using spectral synthesis techniques, we find that its temperature and column density, and area are 9,800 K and  $3 \times 10^{22} \text{ cm}^{-2}$ . Its projected disk size is a remarkably large 100 stellar areas, and the emitting volume resides at a surprisingly large distance of 0.6 A.U. from the star. Surprisingly, we also find that the absorption wings of the strongest optical and UV lines in the spectrum extend to  $\pm 1000 \text{ km s}^{-1}$ , even though the rotational velocity is 300–400  $\text{km s}^{-1}$ . We are unable to find a satisfactory explanation for these extreme line broadenings. HD 110432 and  $\gamma$  Cas share similarly peculiar X-ray and optical characteristics such as high X-ray temperature, erratic X-ray variability on

timescales of a few hours, optical emission lines, and submigrating features in optical line profiles. Because of these similarities, we suggest that HD 110432 is a member of a select class of “ $\gamma$  Cas” analogs.”

*Subject headings:* :

stars: individual (HD 110432) – stars: emission-line, Be – ultraviolet: stars – X-rays: stars

## 1. Introduction

HD 110432 (BZ Cru = HR 4830,  $m_v = 5.3$ ) is a bright variable late-Oe to Be-type star (Houk & Cowley 1975) located in the open cluster NGC 4609 (Feinstein & Marraco 1979) and beyond the southern Coalsack. In recent years this star has attracted considerable attention, resulting in several investigations in the X-ray, ultraviolet, and optical wavelength regimes. In each regime, the star has been found to be unusual. In their classic X-ray survey of potential Be X-ray binary systems, Torrejón & Orr (2001, TO01) found that the star is a hot thermal X-ray source. However, the source does not show pulses, transients, or alternate extended high and low states that are typical of most Galactic X-ray Be stars. The optical spectrum is distinguished by He I, Balmer, and Fe II lines having double-lobed emission profiles (Slettebak 1982). Because the spectrum does not show forbidden Fe lines, nebular lines, or features due to a cool companion, it fails the definition of a B[e] star. The star’s substantially reddened colors and linear polarization have made it an important candidate for ultraviolet and optical for studies of interstellar extinction. In this respect the star’s reddening is unusual and suggests that its observed flux distribution has been altered by circumstellar matter (Meyer & Savage 1981). This conclusion was reinforced by the study of Zorec, Ballereau, & Chauville (2000), who found that the Balmer jump is affected by a presumed Be decretion disk.

In surveying the published data, we have found that HD 110432 displays unusual characteristics even for a Be star, and some of these hint at the coexistence of processes that are ordinarily mutually exclusive. For example, X-ray activity is usually not associated with Be stars with extensive disks because the disks can absorb soft X-rays. In many respects, HD 110432 resembles the optically normal but anomalous X-ray B0.5e star,  $\gamma$  Cas, and herein we will utilize this star for comparison in the optical, UV, and X-ray wavelength regimes. The exposition of this paper proceeds by discussing first the observational and modeling tools §2 used in the analysis and the fundamental parameters of the star §3. We next develop the star’s properties, grouped by wavelength region, both as found previous investigators and in this study (§4-6). In §7 we discuss the likely properties of members of a “ $\gamma$  Cas” class of stars.

## 2. Observations and Modeling Tools

### 2.1. Optical data

In this study we obtain photometric and spectroscopic observations of HD 110432 to investigate whether its optical properties might be related to the X-ray variability. The

photometric observations were carried out by the observing staff of the 0.5-m telescope at African Astronomical Observatory’s Sutherland station during 2002 February 6–May 7. The comparison stars used for these observations were two late-type B stars, HR 4736 and HR 4944. All three stars were observed through the same neutral density filter and standardized with respect to “E-region” UBVRI photometric standards. Our results showed correlated variability among the light curves of all filters. The results for the *V*-band monitoring are shown in Figure 1.

To investigate the properties of the disk and the star’s optical variability over short time scales, we undertook a high resolution spectroscopic campaign on January 26–February 1, 2005). Using the *Giraffe* spectrograph attached to the 1.9-m telescope of the South African Astronomical Observatory (SAAO), we obtained 142 spectra during this week. In a similar manner, Dr. David Laney obtained 61 spectra for us on February 22–March 1, 2005. In both cases the procedure was to place 50 echelle orders on the CCD detector and thus produce a nearly continuous wavelength coverage over the range  $\lambda\lambda 4270\text{--}6290$ . In this configuration the spectroscopic resolution was 32,000,. We obtained signal-to-noise ratios of about 100 per two-pixel resolution element in an exposure time of 10–20 minutes. Ten of the fifteen nights were suitable for discovery of *migrating subfeatures*,, which are discussed below, according to our (somewhat arbitrary) criterion of at least 10 observations distributed over at least three hours of a night.

## 2.2. Spectral synthesis modeling

In §6.2.2 we will discuss results of a number of line syntheses we performed using the *SYNSPEC* code, version 48, written by Hubeny, Lanz, and Jeffery (1994). As input for these solutions, we used the atomic data from the line library (1990) and a standard model atmosphere (Kurucz 1990) having parameters  $T_{\text{eff}} = 24,000$  K,  $\log g = 4$ , and  $\xi = 2$  km s $^{-1}$  and computed spectra every 0.01 Å. We assumed standard abundances for these computations and convolved the result with an Unsold “rotation function” using computed continuum intensities determined for a grid of 20  $\mu$  angles from a vertical direction in the atmosphere. To compute the effect of a circumstellar “cloud” or disk on the spectrum we used the output from our *SYNSPEC* calculation as input for a computation of cloud absorption or emission by the *CIRCUS* program (Hubeny & Heap 1996).

In both these programs we used a working  $V_{\text{rot}} \sin i = 300$  km s $^{-1}$ , but this value need not be known precisely because the narrower emission line contributions can be easily separated from the underlying broad photospheric line absorptions. We ran *CIRCUS* in its LTE reemission mode, that is by evaluating the radiative transfer relations assuming a locally

defined excitation and ionization temperature. Other important disk physical parameters used to compute the equivalent widths of lines formed in the disk are its column density, projected disk area, microturbulence, and chemical composition (assumed herein to be solar). A volumetric particle density of  $10^{11} \text{ cm}^{-3}$  was chosen from the disk model for  $\gamma$  Cas (Millar & Marlborough 1988). Except in one case noted below, we imposed the condition that our model disks were homogeneous. *CIRCUS* handles as many as three clouds with independent velocity and thermodynamic gas parameters. For the case of one exception described below, we utilized this capability and constructed a two-temperature disk model.

In many analyses with these programs, we have had to make educated guesses to set the most important parameter, the disk temperature. In these cases this temperature guess drives the value of most of the other parameters. The same general statement can be made about the optical depth of the lines considered: generally they are optically thick or optically thin. As detailed below, the presence of species in different states of excitation (21 eV lines of neutral helium and lines of  $\text{Fe}^{1+}$ ) together constrain the temperature. The equivalent width ratios of iron lines having different atomic  $gf$  values enabled us to refine the optical depth and the hence emitting region’s mean column density. Because of these circumstances, we were able to constrain the thermodynamic and turbulent parameters to a degree we have not been able to for Be disks in other temperature regimes. However, we should emphasize that while these properties define the total volume of the emitting gas, they do not define its distance from the exciting star, or the geometry of the volume. These parameters are better defined by separate kinematic arguments.

### 3. Fundamental physical properties of HD 110432

Observations of HD 110432’s optical and UV spectrum suggest a spectral type in the range of B0 to B2 (Hiltner et al. 1956, Codina et al. 1984, Ballereau et al. 1995). Although previous distance estimates have run as high as 400–430 pc (Codina et al. 1984), *Hipparcos* parallaxes have led to a more modest value of 300 pc (Perryman 1997). This smaller value suggests that this early B star is only about a magnitude above the main sequence.

Surveys of OB stars have determined that the UV reddening curve of HD 110432 is peculiar (e.g., Meyer & Savage 1981). In their summary of  $E(B-V)$  reddening results for this star in the literature, Rachford et al. (2001) concluded that a “low” value of  $E(B-V) = 0.40$  magnitudes results if the star’s parameters lies within the spectral type and class ranges of B0–B2 and V-III, respectively, and if the reddening toward the star is representative of the average galactic relation. One can reconcile this low  $E(B-V)$  with the value of 0.51 found by Meyer & Savage if one attributes a reddening difference  $\Delta E(B-V) \approx 0.11$  to a circumstellar

nebula or disk near the star.

Zorec, Frémat, & Cidale (2005) have recently calibrated the Balmer jump criteria ( $D$ ,  $\lambda_1$ ) they measure in 97 OB stars to current-generation model atmospheres. This work allowed them to assign values of  $T_{eff} = 23,100$  K and  $\log g = 3.8$  to HD 110432. However, we have found that the strengths of certain UV temperature indicators, such as He II  $\lambda 1640$ , indicate a slightly higher temperature. This is in accord also with the UV-to-near-IR fitting of the star’s spectral energy distribution with a model having  $T_{eff} = 25,000$  K and  $\log g = 3.5$  (see Fig. 1 of Codina et al. 1984). In this paper we will adopt a compromise value of  $T_{eff} = 24,000$  K and a log gravity  $\log g = 4$ , for our line syntheses. We believe that the  $T_{eff}$  is at least this high.

The radial velocity of HD110432 is uncertain because its few strong absorption lines are very broad. An examination of the literature shows determinations ranging from  $+9$  to  $+35$   $\text{km s}^{-1}$ . Because of this scatter, the star is generally noted as being variable in velocity. For example, we note the comment by Thackeray, Tritton & Walker (1973; TTW73): “The H emission lines are very strong, being visible at least as far as H9. The velocities are mainly based on Balmer emission. He absorption is faintly visible (B8 V) and Fe II emission suspected.” We have adopted for this study the most recently determined value of  $+9$   $\text{km s}^{-1}$  by TTW73.

According to the literature, the rotational velocity of HD 110432 has been obtained from either the  $\lambda\lambda 4471\text{--}4481$  optical region or the UV resonance lines. In the first case, various optical studies have attempted to measure the  $V_{rot} \sin i$  from the He I  $4471\text{\AA}$  line. (The often used nearby Mg II  $4481\text{\AA}$  line is hopelessly blended in this star’s spectrum.) These studies have given results in the range of  $300\text{--}380$   $\text{km s}^{-1}$  (Slettebak 1982, Ballereau et al. 1995). However, Zorec, Ballereau, & Chauville (2000) have noted that this line is probably mutilated by reemission and that any velocities derived from fitting this line are open to question. Codina et al. (1984) fit the C IV and Si IV resonance lines with a velocity of  $360$   $\text{km s}^{-1}$ . However, as we will develop below, there appears to be an issue as to whether the components they identified are photospheric. In view of these uncertainties, we obtained the *FUSE* spectrum of this star from the MAST archives. These are displayed in Figure 2. Here we have fit the *FUSE* spectrum with a synthetic spectrum computed with *SYNSPEC* using a rotational parameter  $V_{rot} \sin i = 250$   $\text{km s}^{-1}$ . Additionally, we have fit the profile with a rotational broadening of  $300$   $\text{km s}^{-1}$ , except that in this case we also added emission from a warm circumstellar cloud, with parameters discussed in §6.2.2. Despite these seemingly well determined values, the *FUSE* spectrum actually shows essentially the same broadening for HD 110432 as  $\gamma$  Cas. We have performed a similar exercise for the fitting of the He II  $1640\text{\AA}$  line and the Fe III line-rich region of  $\lambda\lambda 1910\text{--}1930$ . We found a value  $V_{rot} \sin i = 300$

$\text{km s}^{-1}$  in both cases. While these determinations are internally consistent, they are lower than the value of  $\approx 400 \text{ km s}^{-1}$  that Chauville et al. (2001) and Harmanec (2002) have found from fitting optical lines. The disparity with respect to our result is an example of a well-known tendency of UV line analyses to result in lower rotational velocities than analyses of optical lines. The most important result to take away from this exercise is that the velocity is probably *at least*  $300 \text{ km s}^{-1}$ . Whatever its precise value, it is nearly the same as the value for  $\gamma$  Cas.

## 4. X-ray Properties

### 4.1. X-ray characteristics

The *BeppoSax* spectrum analyzed by Torrejón & Orr’s (2001; TO01) indicates that HD 110432 is a hard X-ray source. These authors fit this spectrum using an MEKAL model with a temperature of  $kT = 10.55 \text{ keV}$  or a power law fit with a photon index  $\alpha = 1.77$  and cut-off energy  $E_c = 16.69 \text{ keV}$ . An improved fit with assumed Fe 6.7 and 6.9 keV emission lines is consistent with a thermal fit, and therefore a thermal interpretation is to be preferred. The absorption column density from the attenuation of soft X-ray continuum flux in this model is about  $1.08 \times 10^{22} \text{ cm}^{-2}$ , or fully a factor of ten higher than the ISM column densities inferred from ultraviolet atomic and molecular hydrogen lines (Rachford et al. 2001). This result reinforces Meyer & Savage’s (1981) conclusion that a structure surrounding the star influences its flux distribution over a wide range of wavelengths.

Although a temperature of  $10.55 \text{ keV}$  is a very high temperature for X-ray emitting gas near a Be star, it is nearly identical to the value obtained for  $\gamma$  Cas (e.g., Owens et al. 1999, Smith et al. 2004). A light curve generated from the 5-hour exposure exhibits a dip in flux followed about two hours later by a rise to its initial level. With the permission of the authors, we have reproduced the TO01 light curve in Figure 3. TO01 supposed that the variation in this light curve is periodic and ascribed it to a 4-hour rotation of a hypothetical white dwarf with a spotted surface in a binary system. Although this timescale is consistent with white dwarf rotation, a single modulation is not a convincing demonstration of a period. To show how another interpretation is possible, we depict in Figure 4 an *RXTE* light curve of  $\gamma$  Cas over a comparable stretch of time. This particular time sequence was taken from that shown by Figure 2 of Robinson & Smith (2000), and it is centered at about 10 UT on 1998 November 24. Superimposed on this figure is the sine curve fit obtained by Torrejón & Orr for the HD 110432 data, adjusted for count rate. Clearly, the sine wave is a reasonably good fit to the  $\gamma$  Cas variations. Yet, a glance at the full data train in the Robinson & Smith figure makes it obvious that that “sinusoidal variation” in the  $\gamma$  Cas curve is actually part

of a series of a seemingly meandering temporal pattern that indicates that the appearance of a periodicity is illusory. From this comparison the temporal characteristics of the light curves of HD 110432 and  $\gamma$  Cas are essentially the same. This fact, the moderately high X-ray luminosity, and the like X-ray spectral characteristics prompted us to investigate other attributes that we would expect of a  $\gamma$  Cas analog.

## 4.2. Comparison of long-term X-ray and optical variations

Because both the X-ray temperature and variability properties of HD 110432 are reminiscent of  $\gamma$  Cas, we may look for other possible similarities in terms of published X-ray/optical correlations. We do not yet know the binarity status of HD 110432, but we do know that that  $\gamma$  Cas is a nearly circular binary with a period of 204 days (Harmanec et al. 2000, Miroshnichenko, Bjorkman, & Krugov 2002). However, the mass and evolutionary status of the secondary of  $\gamma$  Cas are unknown. Interestingly, the X-ray flux of  $\gamma$  Cas varies by a factor of three over timescales of months (Robinson, Smith, & Henry 2002; “RSH02”). These variations do not correlate with the binary period but instead are characterized by cyclicity. RSH02 found that variations from several epochal averages correlate very well with a 3% optical variation, and that the amplitude of the variations increases from the Johnson  $B$  to  $V$  filter. Initially, RSH02 found that the cycle length can have a range of 55–90 days. However, continued optical monitoring of  $\gamma$  Cas has revealed that the size of the variations increase into the near-IR wavelength region (Smith & Henry 2005). This work also shows that the cycle lengths can be as long as  $\approx 150$  days.

To see whether HD 110432 exhibits optical characteristics similar to the optical modulations that in  $\gamma$  Cas also correlate with X-ray variations, we undertook the photometric monitoring campaign described in §2.1. Our results showed correlated variability among the light curves of all optical and near-IR filters. In the case of HD 110432, the results for the  $V$ -band magnitudes in Fig. 1a. show that after the start of the monitoring period the star’s optical magnitude faded rapidly by  $3\text{--}3\frac{1}{2}\%$ . After a gap in monitoring of nearly two months, the star once again regained its initial brightness. At the end of the observing season, the star’s faintness faded to its mean level. This variability is typical of a cyclical behavior in Be stars. If this particular cycle is representative of the variability of this star, then the cycle amplitude, waveform, and length are all similar to the optical cycles in  $\gamma$  Cas. In addition, according to the preponderance of scatter in the upper left of the constant-color relation of Fig. 1b, the star’s brightest changes were greater during these variations in the  $V$  band than the  $B$  band. These optical properties are similar to those RSH02 found for  $\gamma$  Cas.



## 5. Ultraviolet properties

From their analysis of two high-resolution, long and short-wavelength *IUE* spectra of HD 110432, Codina et al. (1984) adopted a spectral type of B1 based on the strong photospheric He II  $\lambda 1640$  line. We agree with this analysis and find that this line is only 10% weaker than in the spectrum of  $\gamma$  Cas. This would imply that the effective temperature of HD 110432 is only 1,000–2000 K lower. When corrected for this small difference, the He II profiles in the spectra of these two stars are virtually identical.

Codina et al. also discussed the strong wind absorptions in the blue wings of the resonance lines of C IV, NV, and Si IV. This absorption is punctuated by the presence of DACs (Discrete Absorption Features) in the C IV and Si IV doublets. Figure 5 displays a sample of three *IUE Short Wavelength Prime* camera spectra in the neighborhood of the C IV doublet complex. These examples include the 1981 spectra discussed by Codina et al. as well as an exposure each from the 1986 and 1991 epochs. The addition of spectra from 1986 and 1991 indicates that the wind absorption complex is typically very strong for a Be star, though not inordinately so for a Be star. Likewise, variability is easily visible in the blue wings of the C IV and Si IV resonance lines. Over timescales of years, the DACs exhibit a tendency to recur at approximately the same values (see Fig. 5). Rapid variations are sometimes present at low and high velocities in the C IV and Si IV lines on timescales as short as several hours. These are common characteristics in wind absorptions in ultraviolet spectra of Be stars, and in the spectrum of  $\gamma$  Cas in particular (Cranmer, Smith, & Robinson 2000; CSR00).

Codina et al. determined a rotational velocity from fitting profiles of the C IV and Si IV lines. However, because the centroid radial velocity is about  $-100 \text{ km s}^{-1}$ , we believe that the feature they measured is primarily not photospheric. Rather, it seems to represent a low-velocity DAC feature of the wind. (The profile in question is represented is part of the same spectrum as the solid line in Fig. 5.) To reinforce this point, in Figure 6 we display the mean of two *IUE* spectra in the neighborhood of the Si IV  $1403 \text{ \AA}$  line as a thin solid line. In this spectrum we identify the red wing of the Si IV line as that *most closely corresponding to the photospheric component of this line*. We have also coplotted the mean  $\lambda 4471$  and (offset)  $\lambda 5876$  lines of the optical spectrum discussed in §6.3. The red wings of all these strong absorption feature exhibit a common gradual tapering to the continuum. This fact suggests that the red halves of these ultraviolet absorption lines are primarily formed in a layer having the radial velocity near zero, consistent with their formation in the photosphere.

## 6. Optical high-resolution spectroscopy

### 6.1. Migrating subfeatures

#### 6.1.1. *The migrating subfeatures in line profiles of $\gamma$ Cas*

Yang, Ninkov, & Walker (1988) first pointed out the existence of a peculiar new class of traveling features in the line profiles of  $\gamma$  Cas. These “migrating subfeatures (*msf*) features form in the blue wing and move at a rate exceeding the expected star’s surface rotation rate. They generally form in loose groups, and although they are usually present they can be occasionally absent on any given night. Often an *msf* can form or disappear (or both) during the time it moves across the line profile (Smith 1995). Although Yang, Ninkov, & Walker observed *msf* in optical line profiles, these features have since been observed in high quality time-serial ultraviolet spectra (Smith & Robinson 1999; SR99). Spectral line syntheses of the ultraviolet data suggests that the *msf* are likely to be produced by the absorption caused by intervening clouds forced into co-rotation by putative magnetic fields over the star’s surface (Smith, Robinson, & Hatzes 1998). These are probably the same clouds (or small cloudlets related to them) whose passages produce small variations in the ultraviolet continuum light curve (Smith, Robinson, & Corbet 1998; SRC98). Until this study, *msf* have been reported in the line profiles of  $\gamma$  Cas and only one other star, AB Dor (Cameron-Collier & Robinson 1989). The latter is an active, magnetic pre-main sequence K dwarf (e.g., Hussain et al. 2000).

#### 6.1.2. *Discovery of migrating subfeatures in line profiles of HD 110432*

To investigate whether the line profiles of HD 110432 exhibit any type of rapid variability, we undertook the spectroscopic campaigns in 2005 January and February described above. From the resulting sequences we computed grayscale images from the difference spectra of each nightly mean spectrum. In these computations we first removed cosmic ray events and isolated bright pixels by correcting them to the mean flux of their neighbors. We also removed minor artificial continuum undulations from the initially computed difference spectra by removing a fifth degree polynomial fit.

In our grayscale results for six nights (the fifth of our seven nights in January was largely clouded out), we found clear *msf* patterns for two nights, and these are presented in Figure 7. These patterns were slightly weaker on the third night and weaker still on the fourth and sixth night. By the seventh night no *msf* pattern could be detected. Similarly, of three nights in February having 10 or more observations, *msf* were present on two of them and not

on a third. Note on January 27th (see Fig. 7) the clear three narrow dark features running diagonally toward the upper right part of the grayscale. On January 25/26 one can see that the end of a first, and the beginning of a fourth, *msf*-like feature are present. Additionally, from the figure we estimate an acceleration rate of  $+100 \pm 10 \text{ km s}^{-1} \text{ hr}^{-1}$  for the *msf* features in Fig. 7. Within the errors this value is the same as the rate  $+92 - 95 \text{ km s}^{-1} \text{ hr}^{-1}$  for the *msf* found in line profiles of  $\gamma \text{ Cas}$  (e.g., Smith 1995, Smith & Robinson 1999; SR99).

The presence of small co-rotating clouds anchored to a rapidly rotating star is a necessary condition for the presence of magnetic fields, an inference that cannot be made from zeeman observations. For this reason any claim of detection of *msf* calls for a discussion of mechanisms that might confuse this interpretation. A reminiscent kind of spectral pattern is the traveling “bumps” that are produced on line profiles by high-degree nonradial pulsations (NRP). Although NRP are generally found in cooler spectral types than B1, they have been observed in the O9.5 V stars  $\zeta \text{ Oph}$  and HD 93521 (Reid et al. 1993, Howarth & Reid 1993). Their characteristics in these stars’ spectra can be compared with the description of *msf* for line profiles of  $\gamma \text{ Cas}$ . However, in general the dark striations caused by NRP and by intervening corotating clouds differ in several respects:

- i)* the spacings of *msf* are irregular, such that the time intervals between successive passages can change, while for monoperiodic NRP the bumps are evenly spaced.
- ii)* the absorptions constituting the *msf* are confined to small wavelength intervals compared to the spaces between them. In contrast, the waveforms of monoperiodic NRP are nearly sinusoidal. The dark and line bands in a grayscale depiction have nearly the same width.
- iii)* *msf* can be present on any one night and disappear or appear only sparsely on a second night. The available data suggest that both they and their associated X-ray activity centers have limited lifetimes of only one to a few days (RS99, RSH02). In contrast, the NRP bumps are present every night, and their visibility varies over short timescales only because of the interference of bump systems arising from different modes of comparable strength.
- iv)* the *msf* in HD 110432 and  $\gamma \text{ Cas}$  exhibit accelerations of  $92 - 100 \text{ km s}^{-1} \text{ hr}^{-1}$  whereas the bumps in  $\zeta \text{ Oph}$  and HD 93521 move at a rate near  $150 \text{ km s}^{-1} \text{ hr}^{-1}$ . Either of these rates, but especially the latter one, is higher than would be manifested by a hypothetical fixed dark disturbance on the star’s surface (Smith 1995).
- v)* *msf* seldom last during a full passage from the blue wing to the red wing whereas NRP bumps do so as a rule. High signal-to-noise observations of the UV lines of  $\gamma \text{ Cas}$  (SRC98) indicate that weak *msf* are ubiquitous in spectral regions with a dense packing of lines. These data also indicate that these features can have lifetimes as short as 1–2 hours (SR99).

All of these *msf* attributes defined from  $\gamma$  Cas are met in our observations of HD 110432. However, the first two points listed above are risky discriminators between NRP and *msf* in themselves. For NRP stars with multiple high-degree modes, like  $\zeta$  Oph, the bands *can* sometimes appear at irregular intervals and exhibit white/black striations on grayscale can be violated.

Point *iii*, the occasional absence of features, is more difficult for NRP to mimic, although it could be mimicked if one sampled the line profiles at unlucky times. Even so, it is difficult for us to conceive that this coming and going of features could occur in the NRP interpretation *twice*, as in our January and February monitorings.

According to the data of Reid et al. (1993), the total observing timespan needed to differentiate between NRPs and *msf* on a particular night is about 7 hours. In this timescale, one can begin to decide whether the features are “permanent,” and that they do not disappear either because the intrinsic disturbance dissipates or because an elevated cloud responsible for it moves off the background stellar disk. Our observing durations are too short to provide this type of conclusive test. However, some of our features do disappear or appear suddenly near the middle of the profile, and this suggests short lifetimes.

Our points *iv* and *v* constitute additional arguments that these features are *msf*. This is because in general migrating NRP bumps can have essentially random acceleration values, that is, there is no special association of these rates with the value of an advected surface disturbance. For a rapidly rotating B0.5–B1 IV star, an acceleration of 95–100 km s<sup>−1</sup> hr<sup>−1</sup> of features on line profiles is consistent with co-rotating cloud elevated only well within a stellar radius of the surface. A discovery of co-rotating clouds *close* to a star’s surface is to be favored because of the rapid fall off ( $1/r^3$ ) in magnetic field strength from the surface. The discovery of a star with an even larger magnetic field strength that could confine plasma at higher elevations would be correspondingly less probable, yet it is easy to find such stars, as the discoveries of two O9.5 stars with NRP demonstrate.

We conclude this discussion by stating that it seems highly probable that the time-dependent striations we observe are induced by magnetically confined clouds. However, it is not possible to conclude this definitively conclusion from our grayscale striations on the basis of only several nights of data. The identification of *msf* properties in  $\gamma$  Cas itself has been the result of several investigations of many UV and optical lines. Moreover, it has been possible in the case of  $\gamma$  Cas to trace their occurrences with respect to UV and X-ray patterns (SR99).

## 6.2. The optical emission spectrum

Because the instrumental configurations were static during our January and February observing runs, we could form average spectra from our two datasets. The coadded spectra for both epochs exhibited the same peculiarly shaped emission profiles noted by Slettebak (1982). The only prominent absorption lines in our spectra are the first three Balmer lines and the helium HeI 4471 Å, 5876 Å, and 6678 Å lines. Of these features, only  $\lambda 4471$  is present entirely in absorption. Other light-element lines have absorption wings and the same double-lobed emission cores as the metallic lines. We will discuss the absorption features further in §6.3.

### 6.2.1. Identification and profiles of emission features

HD 110432 has an optical spectrum contains numerous permitted lines in emission. For this reason already it belongs to a small subset of “classical Be stars”<sup>1</sup> with this characteristic. Also, the profiles are unusual because they consist of a flat central emission plateau flanked by stronger *V* and *R* lobes.

We began our analysis by determining the wavelengths of the emission features in the January coaddition spectrum. After correcting for the star’s radial velocity of  $+9 \text{ km s}^{-1}$ , determined by TTW73, we measured the centroid velocities of the features. We found a mean radial velocity of  $+6 \pm 5 \text{ km s}^{-1}$  for the features shown in Fig.8. This agrees well with our adopted velocity for the star.

Next, we identified lines by computing synthesized LTE spectra using the *SYNSPEC* and *CIRCUS* codes. We utilized *CIRCUS* to simulate the effects of a putative circumstellar “cloud” located outside the direct line of sight to the star. The contribution it makes to emission can be computed with an arbitrary doppler velocity. We performed trial computations for models with several temperatures and obtained a good match with the line opacity spectrum computed with  $T = 10,000 \text{ K}$ . The identifications, their excitations, and measured and computed equivalent widths of the *V* and *R* emission lobes are indicated in Table 1. Almost all the lines in the spectrum are Fe II lines, and typically these have excitations of a few eV, as noted in the table. Equivalent widths are not given in the table for those cases for which line strengths are too weak to make a reliable measurement, or for which two or more pairs of *V*, *R* lobes are present because of contributions from neighboring lines. The

---

<sup>1</sup>The spectra of classical Be stars have Balmer emission lines produced by decretion disks. These disks are formed neither by protostellar collapse or binary mass transfer.

He I lines are listed twice, once for the January and February observing runs. A comparison of these entries demonstrates that He I line strengths increased during this interval.

Figure 8 shows a montage of profiles of the He I 5876 Å and 6678 Å lines, as well as a selected group of metallic Fe II lines for both January and February spectra.<sup>2</sup> In aligning the spectra in our montage, we have only had to correct for the star’s radial velocity. The vertical lines in the figure denote the centroid negative and positive velocities of the *V* and *R* peaks. A comparison of these profiles shows that to our ability to measure them, they are identical for lines of any ion. However, small differences are evident from epoch to epoch. First, the February profiles show peaks that are closer together than the January profiles ( $\pm 115 \text{ km s}^{-1}$ , instead of  $\pm 102 \text{ km s}^{-1}$ ). Second, the February emissions represent a 5–10% strengthening over the previous month. An additional property of the red He I lines in both datasets is that the ratio of  $\lambda 5876$  to  $\lambda 6678$  emission equivalent widths is close to 2.0. Since the ratio of the atomic *gf* values for these two lines is 2.5, this value indicates that the He I lines are nearly optically thin. This property is true of the metallic lines as well, according to our simulations below.

### 6.2.2. Analysis of the emission spectrum

The double-lobed structure we observe in the optical spectrum of HD 110432 is the classical shape of an optically thin disk viewed edge-on. Therefore, we have assumed that this is the correct viewing geometry in evaluating the equivalent widths of these lobes. We measured equivalent widths by assuming that the lobes have gaussian cores and symmetric extended wings. We measured their half equivalent widths by measuring their contributions between wavelengths defining the central core of the lobe and the point where the wing merged with the stellar continuum, typically  $50 \text{ km s}^{-1}$  from the line core. In column 4 of Table 1 we list the sum of these values for the *V* and *R* lobes. These are the means of the equivalent widths of these two features. The last column of the table is the computed equivalent width obtained from the  $T = 9,800 \text{ K}$  model defined below. This value is computed by subtracting the narrow contribution of the disk component produced by *CIRCUS* from the rotationally broadened photospheric line given by *SYNSPEC*. Since the observed profiles in Fig. 8 are the same to our errors of measurement, we can evaluate attributes such as the strengths of their emission lobes straightforwardly.

---

<sup>2</sup>We can add from an examination of a few archival spectra obtained with the ESO 3.6-m. Coude Echelle Spectrograph, that certain weak lines (e.g., Fe II 4309 Å) have emission profiles similar to those in our montage.

The analysis of the specific parameters for our homogenous disk model proceeds from the following steps.

*a) Disk Temperature* Lines of neutral helium and  $\text{Fe}^{1+}$  co-exist in the optically thin regime only in a narrow region of temperature. Therefore, we have exploited this fact to use the ratio of the strengths of these lines to determine  $T_{\text{disk}}$ . Using *CIRCUS* models, we found that the number of helium atoms populating their 21 eV levels drops quickly from a moderate finite value at 10,000 K to effectively zero at 9,300 K ( $N_e = 10^{11} \text{ cm}^{-3}$ ), assuming normal chemical abundances. The single temperature that best fits the observed ratios in Table 1 is  $9,800 \pm 200 \text{ K}$ . The error bars on this figure are determined as much by our lack of precise knowledge of the volumetric electron density as by photometric or measurement measurement errors.<sup>3</sup>

*b) Column density:* The measured equivalent width ratio of the helium lines  $\text{EW}(\lambda 5876)/\text{EW}(\lambda 6678) = 2.0$  provides a good estimate of the degree of optical thinness. Knowing the disk temperature, we computed models with varying column densities until we found one that matched this value. With the column density computed, we divided this value by the assumed mean volumetric density to determine the mean disk thickness along the line of sight in kilometers (this value is only as good as our assumed  $N_e$ ).

*c) Microturbulence:* This value was determined by matching the ratios of Fe II lines having the same excitations but comparatively low and high  $gf$  values, e.g.  $\lambda 4923$  and  $\lambda 5018$ . The value determined from these ratios in our line syntheses is  $\xi = 10 \pm 3 \text{ km s}^{-1}$ .

*d) Projected area:* Finally, the strength of absorption or emission lines sets the projected star disk in natural units of a star area,  $\pi R_*^2$ . Note that all other quantities outlined in *a-c* utilize line strength *ratios*. The projected area we determine from our *CIRCUS* models is the value used to match the *absolute* computed strengths to the observed ones (columns 4 and 5 in Table 1).

As a clarification, we should note that the solution described above represents a volume-weighted mean for the portion of the assumed homogeneous disk we have considered. To be more precise, it is the portion at maximum elongation (i.e., in the plane of the sky), and not even the disk component contributing to emission in the plateau of our profiles. A more realistic approach to modeling the disk segment in the sky plane might take into account that the disk temperature and hence the He I/Fe II emission should vary with distance from the star. To evaluate the effects of a temperature gradient, we fit several lines in Table 1 with a *two-temperature* component solution, that is with two distinct but equal volumes having the

---

<sup>3</sup>We believe that the poor fit for the Fe II 6318 Å may be due to inaccurate atomic data for this line.

same column densities and arbitrarily chosen temperatures of 10,000 K and 9,000 K. (Since these temperatures are chosen arbitrarily, the distances of the two components to the star are left unknown). We also scaled the areas of the two equal-area components until they fit the He I and Fe II lines in the table to the same precision as our first model. We found a good match when the two subareas were 37 stellar areas each. This exercise is not meant to show merely that adding an additional set of parameters to our model fits the data any better than the homogeneous disk case – indeed, we have no basis for preferring one model over the other. Rather, this second model demonstrates that a two-temperature disk reduces the derived large area from 100 to 74 stellar areas, or only 26%. We can conclude that the large areas in our solutions do not seem to be strongly determined by radial temperature gradients through the disk.

A second important point to come out of our analysis relies on a kinematical argument. If the velocity separation of the  $V$  and  $R$  lobes is Keplerian, the volume of the disk in which they must be formed is about 0.6 A.U., assuming a stellar mass of  $12 M_{\odot}$ . This leads us to consider whether the temperature we have derived, 9,800 K, is reasonable for the disk of a B1e star. As a comparison, we may start with the parameters for the disk of  $\gamma$  Cas. In their theoretical analysis of the radiative energy loss/gains of this star’s disk, Millar & Marlborough (1998) found a density-weighted mean temperature of 10,800 K. This determination is in good agreement with the value of  $9,500 \pm 1000$  K that Hony et al. (2000) derived in their analysis of the bound-free absorption edge of the hydrogenic Humphreys jump in infrared spectra. However, this emission is formed primarily within a few stellar radii from the surface of  $\gamma$  Cas. Since Millar & Marlborough’s results indicate that the disk temperature decreases slowly with stellar distance, an extrapolation of their model out to  $\approx \frac{1}{2}$  A.U. would certainly predict a lower value than we have found, even though  $\gamma$  Cas is likely to be the hotter of the two stars. In this event, it may be that nonradiative heating is required to maintain the temperature of the HD 110432 disk.

Third, we note that our disk dimensions, especially an extension out of the plane, do necessarily agree with those of other well studied stellar disk systems. In particular, Be disks originating from decretion or protostellar collapse have densities that are strongly confined to the equatorial plane, and their contours flare outward from the plane. The well studied disk of  $\gamma$  Cas is a case in point. Observations show that the electron density in the plane of this star’s disk is  $\sim 10^{12} \text{ cm}^{-3}$  (Telting 2000), and the column density in the poloidal direction is about  $10^{23} \text{ cm}^{-2}$  (Millar & Marlborough 1998). Interferometric observations in H $\alpha$  light find that hydrogen is ionized out to a radius of about  $6R_*$  (Quirrenbach et al. 1997). A comparison with this detailed description does not allow much leeway to extend the disk of HD 110432 in the radial direction by analogy, since the column density must be low enough for the emission lines to be optically thin, perhaps only  $\sim 1 \times 10^{22} \text{ cm}^{-2}$  when observed along



a radial line of sight. The fact that the  $V/R$  ratio is about one, and moreover that this ratio is nearly constant over a timescale of a month, is consistent with an axisymmetric density distribution in the plane. Then, the only effective way to realize a large projected area is to invoke a geometry in which the disk flares outward from the plane by several  $R_*$ . We trust that this apparent peculiarity will turn out to be a clue to resolving how this star’s disk is maintained.

As a fourth consideration, the question arises whether similar emission features might also be present in the  $\gamma$  Cas spectrum. In fact, Bohlin (1970), Slettebak (1982), and probably TTW73 have already noted Fe II emission lines, including the first two Fe II entries in our table. Bohlin’s paper also referenced to the identification of iron emission lines by Baldwin (1942) and Marlborough & Cowley (1968). moderate-dispersion photographic plates. In the intervening time, it appears that neither the strengths nor the shapes of these features have been studied in the  $\gamma$  Cas spectrum. On the basis of our analysis of the HD 110432 spectrum, we can predict that future observations of the optical spectrum will disclose numerous emission lines with plateau-shaped profiles. Since  $\gamma$  Cas presents an intermediate observing angle, it is not clear that its emission line profiles will include a well-resolved lobe structure, although this may turn out to be true. In any case, the fact that the lines are present in the  $\gamma$  Cas spectrum confirms our picture that the lobe-structure in the HD 110432 spectrum can be attributed to Keplerian rotation of a disk.

### 6.3. The Absorption lines of HD 110432

#### 6.3.1. Description

The only optical line entirely in absorption in our spectra is He I 4471 Å. In Be stars the nearby Mg II 4481 Å line is generally easily identifiable, despite its position in the red wing of the He I feature. In our spectrum the Mg II feature has been multilated by a particularly strong red wing of He I. The wings of this line are broadened symmetrically to at least  $\pm 1000$  km s<sup>-1</sup>. This smearing is shown for the He I  $\lambda 4471$  and  $\lambda 5876$  lines in Fig 6. This broadening is not likely to be instrumentally induced for two reasons. First, as shown in this figure, the extended wing appears to be shared on the uncontaminated long-wavelength side of the Si IV  $\lambda 1403$  line. Second, we may assess the reliability of the continuum and echelle blaze functions by comparing the echelle order ( $m = 45$ ) containing the  $\lambda 4471$  line with the instrumental continua of the two neighboring echelle orders ( $m = 44$  and  $46$ ). In Fig. 6 this spectrum and its associated internal errors are labeled by the annotation "Continuum." The key point of this comparison is that fluxes of the latter orders are flat across the central region of the blazes. Therefore, there is good reason to believe that the broad wings of  $\lambda 4471$  are not

artifacts of a poorly constrained instrumental function.

It is important to note that the core depth  $\lambda 4471$  in our spectra is 10 %. This is a nominal depth for this line in spectra of rapidly rotating early-type Be stars, as we have verified by comparing the corresponding line profiles of  $\gamma$  Cas (Ballereau et al. 1995) and other rapidly rotating B0-2V stars in the UVES Paranal spectral atlas (Bagnulo et al. 2003). Rotational broadening dominates the shape of the (weak) far wings in the latter cases. Our spectral syntheses modeling of the hydrogen and helium lines verifies that this should be the case for stars near the main sequence. For this reason the absorption lines should be characterized as *strengthened* as well as anomalously broadened.

A final interesting property of the “excess broadening” of the strong absorption lines is that the *IUE* spectra which also seem to show them were obtained nearly a decade before the SAAO observations in 2005. Although we would like to conclude that the too-broad line character is present all the time, we must point out that the line profile of  $\lambda 4471$  observed in 1990 by Ballereau et al. (1995) does *not* clearly show the excess broadening. Therefore, this characteristic may not be permanent.

### 6.3.2. What is the broadening agent?

In any context the presence of the strong absorption lines broadened by more than twice the star’s likely rotational velocity presents an interpretational challenge. These absorption lines cannot arise from the blended superposition of two components of a double-lined binary because this circumstance would not produce the substantially strengthened lines we observe. Moreover, spectra of a presumed near edge-on Be-binary system should exhibit radial velocity variations within a few days, and these have not been observed. Such lines in any case might be smeared at suitable epochs but would not be strengthened.

The star’s parallax is in agreement with its spectroscopic luminosity class, so it is not really possible for a compact star such as a white dwarf to dominate the flux contribution of the B star and produce Stark broadened wings. Even so, it is instructive to note what the line profiles of He I lines of DB white dwarfs look like. In consulting the literature, we find it is comparatively easy to find examples of  $4471 \text{ \AA}$  profiles that are Stark broadened to considerable degrees (Wesemael et al. 1993, Liebert et al. 2003). However, many of these same spectra exhibit no visible He I red lines. The red lines of two sdB stars exhibit very weak wings (Heber & Edelmann 2004). Among five DB stars observed by Wolff et al. (2002), only one of them has spectral line wings that extend to  $\pm 350 \text{ km s}^{-1}$ . We can conclude that since the Stark components are weak in the red lines of all these sdB and DB stars, the

excess broadening we see is not caused by pressure broadening. This conclusion is likely to extend to the other broadened lines in the blue spectral region.

Electron scattering can also broaden lines over a velocity range characteristic of the temperature in a hot gas. However, this mechanism is conservative in the sense of redistributing monochromatic flux rather than a strengthening of a line. In any case, for electron scattering to be effective the required very high column densities ( $10^{24-25} \text{ cm}^{-2}$ ) are not present near HD 110432, either in our optical emission line analysis or as inferred from the gradient of the X-ray continuum (TO01).

By process of elimination, we are left with invoking doppler velocities to explain the excess absorption line widths. Before venturing into clearly risky territory, we should pause to remind the reader of our result that the broadening and strengthening properties affect only those lines that are strong and which arise from ions that are relatively numerous in the mid- and upper photosphere. Thus, lines in the far-UV, which are primarily formed in the lower photosphere due to the transparency of the continuum in these wavelengths, are not much affected by conditions in the upper atmosphere. This reasoning leads to the potential explanation that the broadening occurs in a medium located in the upper atmosphere or just above it, where, for example, the UV radiation field must still be strong enough to populate 21 eV levels of neutral helium atoms but is not so strong as to populate the more ionized helium. In order to both strengthen and broaden these lines, the putative velocities of about  $\pm 1000 \text{ km s}^{-1}$  would then serve as a very energetic microturbulence.

Where and how this or any other postulated agent might operate is entirely open to conjecture. If we take the presence of migrating subfeatures as evidence of magnetic control of gas motions, we might conjure up images of magnetically guided arcades of loops, conceivably driven by radiative acceleration. However, a possible problem with this picture is offered by the wind properties of the magnetic O-type star, ( $\theta^1$  Ori C). This star produces a strong radiation field that drives a wind circulation in closed loops (Smith & Fullerton 2005, Gagné et al. 2005), but even for this hot star the flow velocities do not exceed a few hundred  $\text{km s}^{-1}$ . Another argument in favor of the magnetic idea that the energies responsible for the generation of X-rays are sufficient to accelerate gas particles to more than a thousand  $\text{km s}^{-1}$ . However, we cannot suggest how the high energies might be degraded to turbulence, particularly close to the star’s surface, without quickly being transferred to thermal motions.

## 7. Conclusions

HD 110432 is an unusual Be star, whether studied in the X-ray, ultraviolet, or visual regimes. Its hard X-ray spectrum is probably thermal, and as shown in Figs. 3 and 4, its optical light curve shows modulations which arguably are similar to those observed in  $\gamma$  Cas. This makes HD 110432 a fascinating target because it makes its association with the highly enigmatic  $\gamma$  Cas possible. The underlying photospheric component of the UV resonance lines is hard to discern, but this component too may be highly broadened. The hydrogen and helium line absorptions of the *Giraffe* spectra obtained in January and February 2005 appear to be “almost photospheric.” These lines suggest a  $\approx$ B1 spectral type that is consistent with the spectral energy distribution determined by Codina et al. (1984). However, the wings of these lines are strengthened by a broadening corresponding to  $\pm 1000$  km s $^{-1}$ . The cause of this broadening is unknown.

A number of metallic emission lines chiefly due to Fe II are present in the green-red spectrum. These features exhibit a central plateau flanked by two  $V$  and  $R$  emission peaks. In addition, at least the first three members of the hydrogen Balmer series as well as the “red” He II lines, exhibit central emissions with this same profile. The  $V$  and  $R$  peaks of all these lines are separated by about 200 km s $^{-1}$ . Both the separation velocity and the strengths of the features can vary on the timescale of a month. We can conclude from the shape of the emission line profiles, the equivalent width ratio of the features in the two “red” He I lines, and the example of the emissions in the  $\gamma$  Cas spectrum, that the emission lobes are formed about  $\frac{1}{2}$  A.U. from the star in an optically thin, Keplerian disk. Using this geometric model, we can solve for the parameters of a homogeneous disk. Along the sight line of maximum elongation of the projected disk edge, the disk temperature is about 9,800 K, the column density along the sight line of maximum elongation of the projected disk edge is  $3 \times 10^{22}$  cm $^{-2}$ , and the projected area is nearly 100 stellar areas. The latter value is quite large and suggests that the disk flares from the central disk plane. The computed disk area can be reduced slightly by assuming that the disk has a temperature gradient. At a distance of  $\approx \frac{1}{2}$  A.U. from the star, a gas temperature of 9800 K may be difficult to maintain from the star’s radiative flux alone. Thus, it is possible that an additional heating source is required.

The X-ray and optical properties of HD 110432 exhibit close similarities with  $\gamma$  Cas, a fact that suggests that the production mechanism of the X-rays may well be the same for these two stars. They are both early-type stars near the main sequence with a high rotation rate, even for a Be star. As for the X-ray properties, both have circumstellar plasma with a temperature of about  $10^8$  K. We can also hazard the prediction that, as with  $\gamma$  Cas, future high quality X-ray light curves of HD 110432 will show nearly continuous flaring. Both

are particularly rapidly rotating Be stars, and both have well developed disks and exhibit strong wind activity and attributes of disk evolution. Our photometric campaign in 2002 has revealed variations in an optical light curve for that suggest a cyclical variation of roughly 130 days. This is consistent with the optical cycles of  $\gamma$  Cas, which range from 55 to 150 days. In both stars, the modulation amplitude increases with wavelength. In addition, from an analysis of a spectroscopic time series, we have found that on several nights the red He I lines exhibit traveling absorption features running through the profiles at a rate equal to the *moving subfeatures* often visible in the profiles of  $\gamma$  Cas. Such features are highly unusual in Be stars, and indeed so far are known otherwise only in  $\gamma$  Cas itself. Their existence is best, though not uniquely, explained by absorptions of small clouds that are locked into co-rotation by surface magnetic fields.

From these observations we suggest that HD 110432 is the first new member of what may be called a “ $\gamma$  Cas class” of X-ray Be stars, so far consisting of two stars. In the case of  $\gamma$  Cas, the prevailing evidence is that these X-rays are produced in the immediate vicinity of the Be star itself, perhaps by magnetic disk-star interactions (RSH02). Whatever the physical site, we may begin to evaluate candidate X-ray production mechanisms by examining the properties of both the X-ray and the star among members of this new class. Moreover, the greater the number of stars amassed in this class, the greater will be the probability of catching disk changes as they occur, and thus of determining the relevance of the disk to the high X-ray emission.

In assessing differences in phenomenology that might be observed in  $\gamma$  Cas and HD 110432, the aspect angle to the observer could play an important role. According to interferometric studies of  $\gamma$  Cas (e.g., Quirrenbach et al. 1997), the star-disk system is observed from an intermediate obliquity. Smith et al. (2004) found that its *Chandra* continuum spectrum is attenuated at longer wavelengths and thus a two column-density model is required the flux distribution. If the X-rays arise from a star-disk interaction, this model fits in well with the expectation that these emission would be emitted from two volumes, one primarily in front of the disk along the line of sight and the other behind it. If one were to observe  $\gamma$  Cas or an equivalent Be star from an edge-on orientation, and further, were to assume that most of the emission occurs outside the disk plane, then one might expect the continuum to be fit to a single column-density model. Yet, a change in observer aspect should leave the line spectrum essentially unchanged. Interestingly, T001 found an intermediate column density of  $10^{22} \text{ cm}^{-2}$ . This figure is consistent with the X-ray active centers residing in an extended region that is not strongly confined toward the equatorial plane. A high-resolution spectrum should be able to address this question further and lead to constraints on the geometry of the formation region and thus the mechanism for the anomalous X-ray emission. Proceeding in the opposite direction, an understanding of disk dynamos could lead to an understanding

of conditions in the inner disk (“disk seismology”).

This paper could not have been written without help from a number of colleagues who provided us with information and encouragement to unravel peculiar properties of this star. Thanks are due first to Dr. J. Torrejón for his generous permission to utilize the light curve figure from the TO01 paper. We also acknowledge a number of helpful discussions about the properties of this star by Drs. Alex Fullerton, Steve Howell, Ted Snow, and Janez Zorec. We gratefully acknowledge the fruitful efforts of Mr. Francois van Wyk, who carried out the photometric monitoring on HD 110432 in 2000 and of Dr. David Laney who kindly obtained many spectra of this star during 2005 February. The quality of this paper was significantly enhanced from comments by an anonymous referee.

## REFERENCES

- Bagnulo, S., Cabanac, R., Jehin, E., Ledoux, C., & Melo, C. 2003, “The UVES Paranal Observatory Project,” [http://www.sc.eso.org/santiago/uvespop/field\\_stars\\_uptonow.html](http://www.sc.eso.org/santiago/uvespop/field_stars_uptonow.html)
- Baldwin, R. B. 1942, *Sky & Telescope*, 1, No. 9, 5
- Ballereau, D., Chauville, J., & Zorec, J. 1995, *A. & A. S.*, 111, 423
- Bohlin, R. C. 1970, *ApJ*, 162, 571
- Cameron-Collier, A., & Robinson, R. D. 1989, *MNRAS*, 236, 57
- Chauville, J., Ballereau, D., Morrell, N., Cidale, L., & Garcia, A. 2001, *A. & A.*, 378, 882
- Codina, S. J., de Freitas Pacheco, J. A., Lopes, D. F., & Gilra, D. 1984, *A. & A.*, 57, 239
- Cranmer, S. R., Smith, M. A., & Robinson, R. D. 2000, *ApJ*, 537, 433
- Feinstein, A., & Marraco, H. G. 1979, *AJ*, 84, 1713
- Gagné, M., Cohen, D. H., Owocki, et al. etc *ApJ*,
- Harmanec, P., Habuda, P. et al. 2000, *A. & A.*, 364, 85
- Harmanec, P. 2002, *Exotic Stars*, ASP Conf. Ser., 279, 221
- Heber, U., & Edelman, H. 2004, *Astrophys. & Sp. Sci.*, 291, 341
- Hiltner, W. A., Garrison, R. F., & Schild, R. E. 1969, *ApJ*, 157, 313
- Hony, S., Waters, L. B., Zaal, P. A. et al. 2000, *A. & A.*, 355, 187
- Houk, N., & Cowley, A. P. 1975, *University of Michigan Catalog of Two Dimensional Spectral Types for the HD Stars*, Ann Arbor: Univ. of Michigan
- Howarth, I. D., & A. H. N. Reid 1993, *A. & A.*, 279, 148
- Hubeny, I., Lanz, T., & Jeffery, S. 1994, *Newslett. Anal. Astron. Spectra*, 20, 30
- Hubeny, I. 1996. & Heap, S. R. 1996, *ApJ*, 470 1144
- Hussain, G. A., Donati, J. F., Collier-Cameron, A., & Barnes, J. R. 2000, *M.N.R.A.S.*, 318, 961
- Kurucz, R. L. 1990, *Trans. IAU*, 20B, 169 and <http://kurucz.harvard.edu/atoms/AEL>
- Kurucz, R. L. 1993, *ATLAS9 Stellar Atmospheres and 2 km s<sup>-1</sup> Grids*, Kurucz CD-ROM #13
- Liebert, J., Harris, H. C. et al. 2003, *AJ*, 126, 2521
- Marlborough, J. M., & Cowley, A. P. 1968, *PASP*, 80, 42
- Meyer, D. M., & Savage, B. D. 1981, *ApJ*, 248, 545

- Millar, C., & Marlborough, J. M. 1998, *ApJ*, 474, 715
- Miroshnichenko, A., Bjorkman, K., & Krugov, V. 2002, *PASP*, 114, 1226
- Owens, A., Oosterbrock, T., Parmar, A., Schulz, R., Stöwe, J., & Haberl, F. 1999, *A. & A.*, 348, 148
- Perryman, M. 1997, *The Hipparcos and Tycho Catalogues*, ESA SP-1200 (Noordwijk: ESA)
- Quirrenbach, A., Bjorkman, K. et al. 1997, *ApJ*, 479, 477
- Rachford, B. L., Snow, T. P. et al. 2001, *ApJ*, 555, 839
- Reid, A. H., Bolton, C. T. et al. 1993, *ApJ*, 417, 320
- Robinson, R. D. & Smith, M. A. 2000, *ApJ*, 540, 474
- Slettebak, A. 1982, *ApJS*, 50, 55
- Smith, M. A. 1995, *ApJ*, 447, 812
- Smith, M. A., Robinson, R. D., & Corbet, R. H. D. 1998, *ApJ*, 503, 877
- Smith, M. A. & Robinson, R. D. 1999, *ApJ*, 517, 866
- Smith, M. A., Cohen, D. H., Gu, M. F., Robinson, R. D., Evans, N. R., & Schran, P. G. 2004, *ApJ*, 600, 972
- Smith, M. A., & Fullerton, A. W. 2005, *PASP*, 117, 13
- Smith, M. A., & Henry, G. W., 2005, in preparation.
- Smith, M. A., & Robinson, R. D. 1999, *ApJ*, 517, 866
- Smith, M. A., Robinson, R. D., & A. P. Hatzes 1999, *ApJ*, 507, 945
- Smith, M. A., Robinson, R. D., & Corbet, R. H. D. 1998, *ApJ*, 503, 877
- Smith, M. A., Robinson, R. D., & G. W. Henry 2002, *ApJ*, 575, 435
- Smith, M. A., & Robinson, R. D. 2003, in *ASP Conf Ser.* 292, *Interplay between Periodic, Cyclic, and Stochastic Variability*, ed. C. Sterken (San Francisco: ASP), 263
- Smith, M. A., Cohen, D. H. et al. 2004, *ApJ*, 600, 972
- Telting, J. H., 2000, in *ASP Conf Ser.* 24, *The Be Phenomenon in Early-Type Stars*, ed. M. Smith, H. Henrichs, & J. Fabregat, 422
- Thackeray, A. D., Tritton, S. B., & Walker, E. N. 1973, *Mem. Royal Astron. Soc*, 77, 199
- Torrejón, J. M., & Orr, A. 2001, *A. & A.*, 377, 148
- Wolff, B., Koester, D., et al. 2002, *A. & A.*, 388, 320
- Yang, S., Ninkov, Z., & Walker, G. A. 1988, *PASP*, 100, 233



Wesemael, F., Greenstein, J. L. et al. 1993, ApJ, PASP, 105, 761

Zorec, J., Ballereau, D., & Chauville, 2000, in The Be Phenomenon in B Stars, ed. M. Smith, H. Heinrichs, & J.

Zorec, J., Frémat, Y., & Cidale, L. 2005, A. & A., in press

### Figure Captions

Fig. 1.— Panel *a* shows the Cousins V-band light curve of HD 110432 during 2002 February–June. If this variation is a cycle, it has a length of perhaps 130 days. Panel *b*) shows a scatter diagram of the V- and R-band variations for the monitoring shown in panel *a*. The reference for the points in the upper left of panel *b* indicates that the optical variations are slightly larger for the V-band than the B-band.

Fig. 2.— A *FUSE* spectrum of HD 110432 and a spectrum of  $\gamma$  Cas shown for reference. The thick dashed line is a scaled synthetic spectrum computed with *SYNSPEC* and broadened by a rotational quasi-convolution of  $250 \text{ km s}^{-1}$ . A thin dashed line also shown represents a similar synthesis computed for both the photosphere and a surrounding warm circumstellar disk, broadened with a rotational velocity function of  $300 \text{ km s}^{-1}$ .

Fig. 3.— A 5-hour *BeppoSax* light curve of HD 110432 constructed by Torrejon & Orr (2001). The solid curve is a 4-hour sine wave fit to the dip in the middle of the observations *By permission of Astronomy & Astrophysics*.

Fig. 4.— A *RXTE* light curve of  $\gamma$  Cas from a 6-hour section of the *RXTE* light curve obtained on 1998 November 25–26; the solid line is the sine curve from Fig. 3. Its amplitude and period are the same as in the first case. Only the mean flux level of this curve has been modified to fit the  $\gamma$  Cas flux.

Fig. 5.— Sample observations of the profile of the CIV doublet complex for epochs in 1981, 1986, and 1991. Rest wavelengths of the two CIV lines and the SWP observing sequence numbers are indicated.

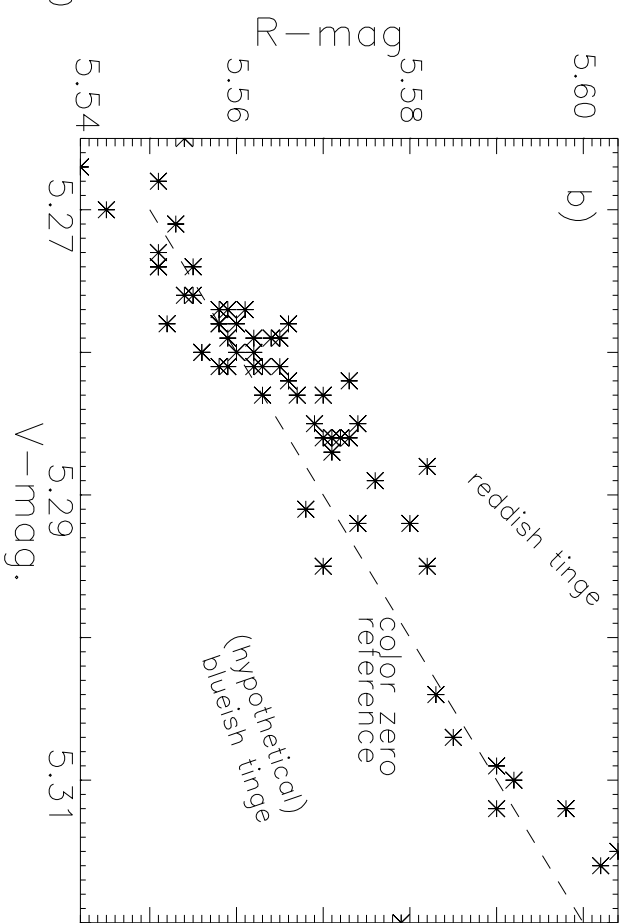
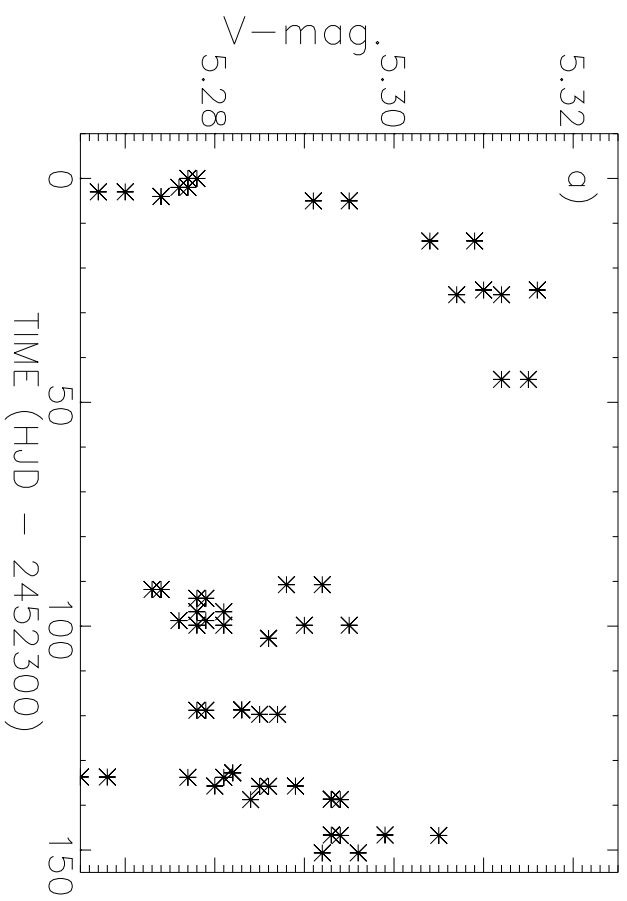
Fig. 6.— A comparison with respect to velocity of the profiles of the He I 4471 Å and 5876 Å lines from our January 2005 *Giraffe* observations with the mean of two *IUE* observations of the Si IV 1403 Å obtained on March 21, 1986 (SWP27970 and SWP27972; this observation coincides with the solid line spectrum shown in Fig. 5). In this figure the He I lines have been suitably scaled in flux to almost match the *IUE* spectrum. The "Continuum" line is the mean spectrum of the two neighboring echelle orders of the *Giraffe* order  $m = 45$  containing 4471 Å. The dotted spectra just below and above this spectrum traces each of the neighboring orders.

Fig. 7.— Grayscale difference spectra of the He I 6678 Å line of HD 110432 on the dates indicated; starting times are 23:00 U.T. and 23:15 U.T., respectively. Limits of  $\pm 330 \text{ km s}^{-1}$  of the line profile are indicated as the approximate extent of the rotationally broadened component of the absorption profile.

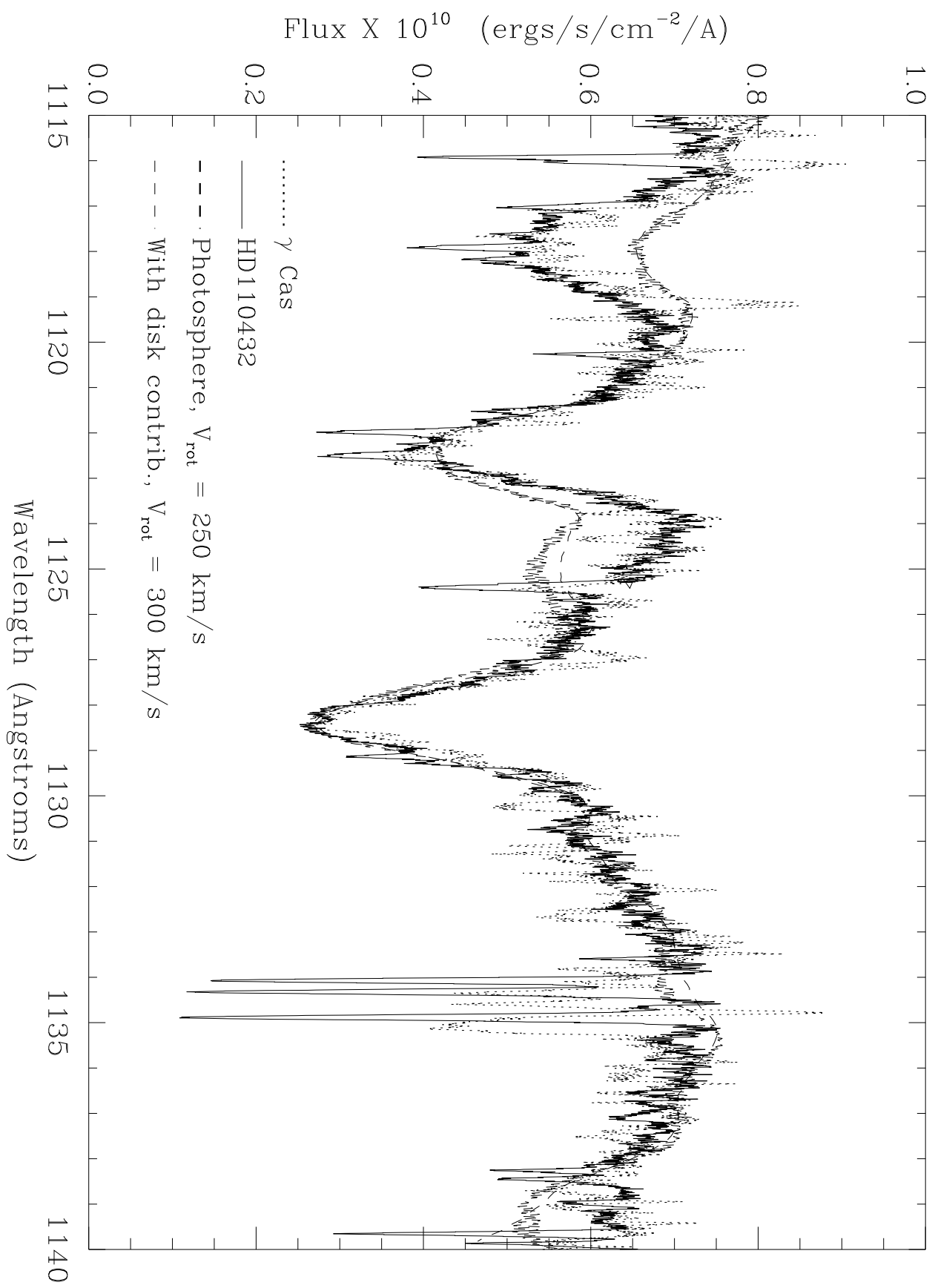
Fig. 8.— Montage of He II and Fe II line emission profiles from the mean spectra of the January and February, 2005 monitoring campaigns. The dashed and dotted vertical lines denote the mean separation of the *V* and *R* emission lobes for the January and February datasets.

Table 1: Emission Line Identifications and Strengths

Ion	Wavelength (vac.)	$\chi$ (eV)	Observed EW (mÅ)	Computed EW (mÅ)
S II	4524.68-.94	15.5		
Fe II	4555.89	2.8		
Fe II	4583.84	2.8	-0.182 $\pm$ .032	-0.182
Fe II	4629.34	2.8	-0.076 $\pm$ .011	-0.058
Fe II	4666.76	2.8	-0.080 $\pm$ .015	-0.056
Fe II	4923.93	2.9	-0.101 $\pm$ .004	-0.103
Fe II	5018.44	2.9	-0.252 $\pm$ .026	-0.312
Fe II	5169.03	2.9	-0.264 $\pm$ .008	-0.258
Fe II	5197.58	3.3	-0.150 $\pm$ .007	-0.137
Fe II	5234.62	3.2		
Fe II	5276.60	3.2	-0.164 $\pm$ .028	-0.190
Fe II	5284.07	10.5		
Fe II	5316.62	3.2	-0.236 $\pm$ .030	-0.217
S II	5362.87	3.2	-0.122 $\pm$ .002	-0.090
Fe II	5534.89	10.5		
He I	5875.62	21.1	-0.304 $\pm$ .004	-0.300
He I (Feb.)	5876.62	21.1	-0.361 $\pm$ .004	
Fe II	6247.55	3.9		
Fe II	6317.98	5.5	-0.161 $\pm$ .051	-0.043
Si II	6347.11	8.1		
Fe II	6456.38	3.9	-0.145 $\pm$ .024	-0.118
He I	6678.15	21.2	-0.146 $\pm$ .003	-0.150
He I (Feb.)	6678.15	21.2	-0.199 $\pm$ .013	



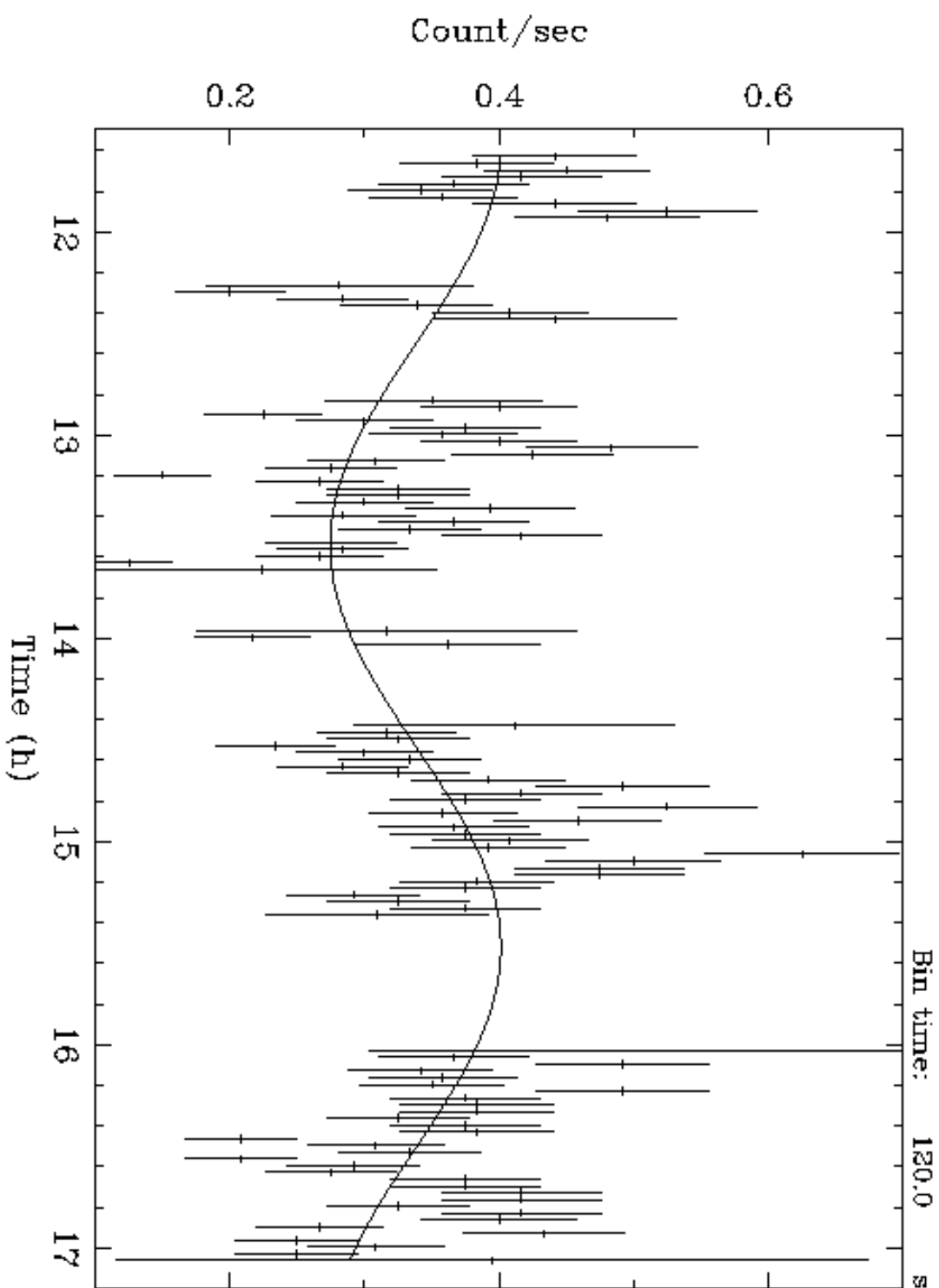




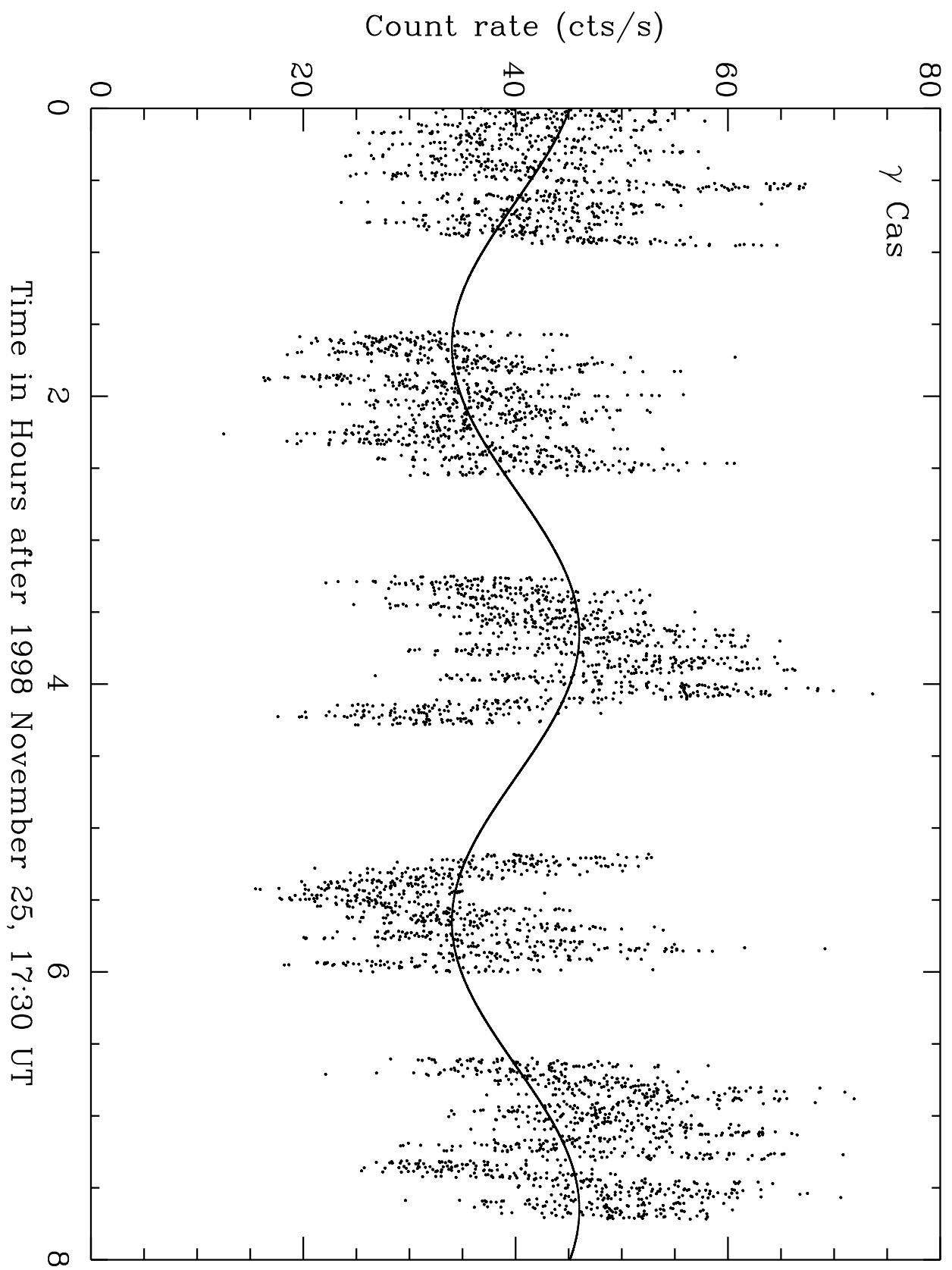




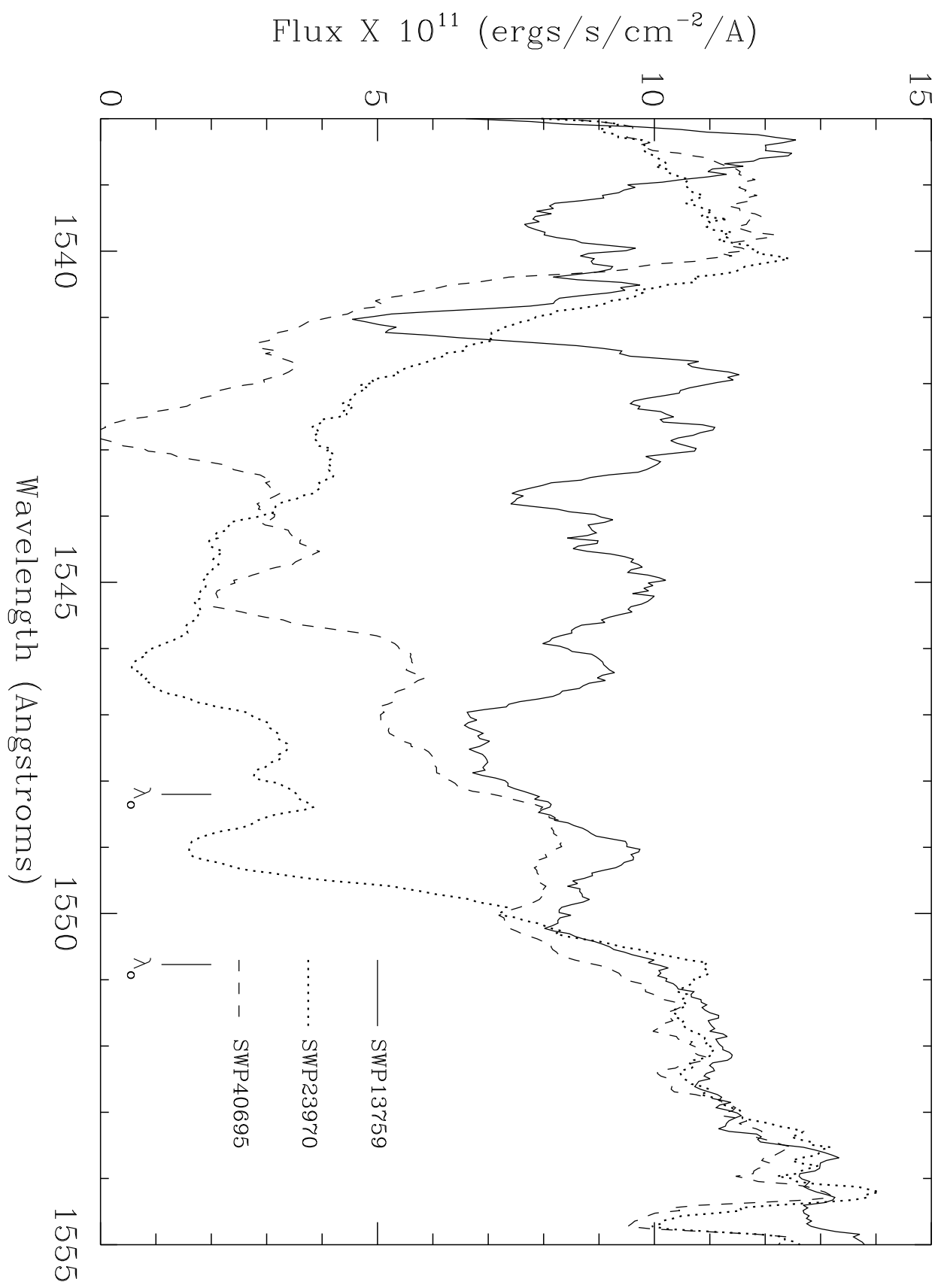
HD 110432



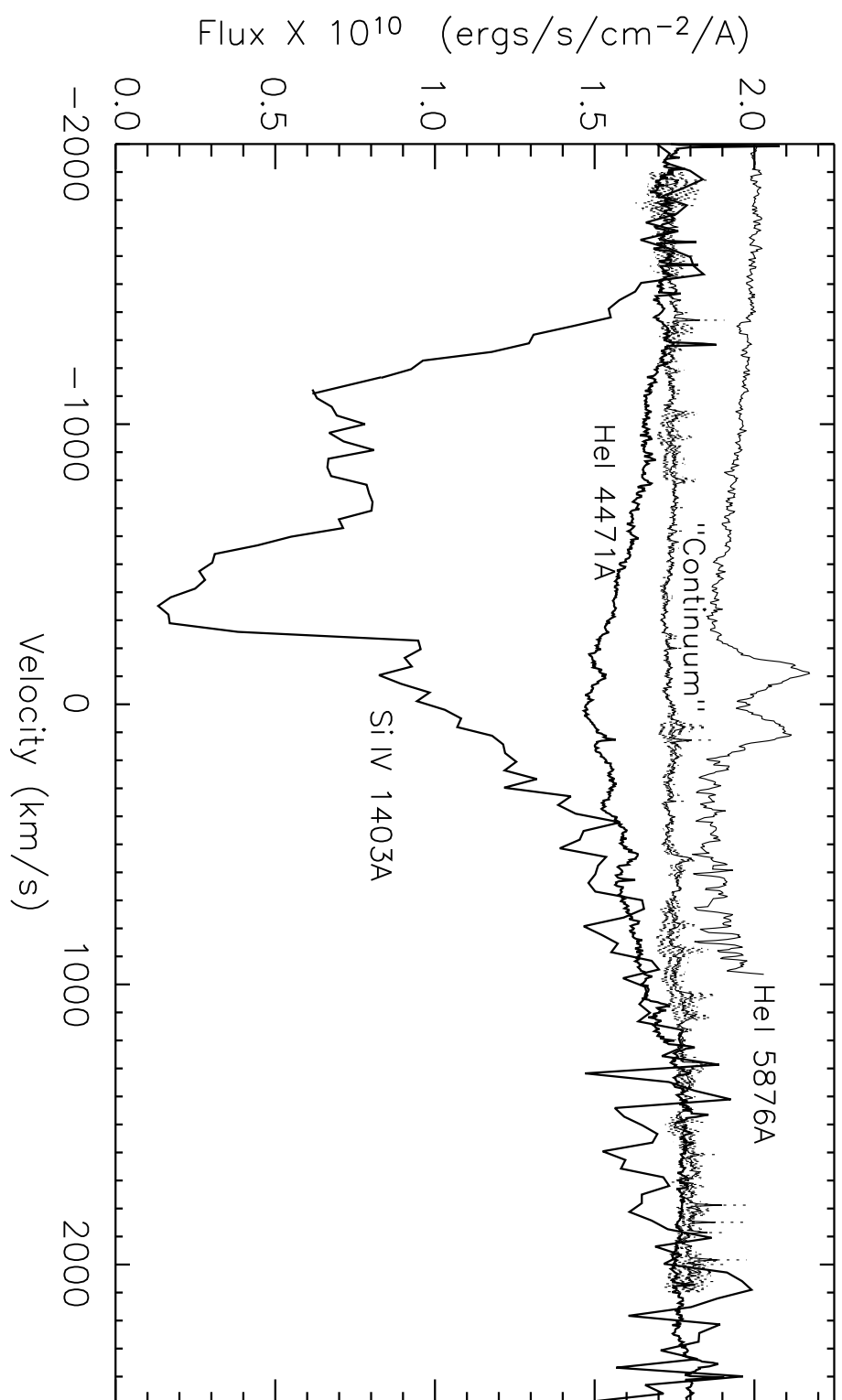
Start Time 10462 11:37:46:665 Stop Time 10462 17: 3:46:665





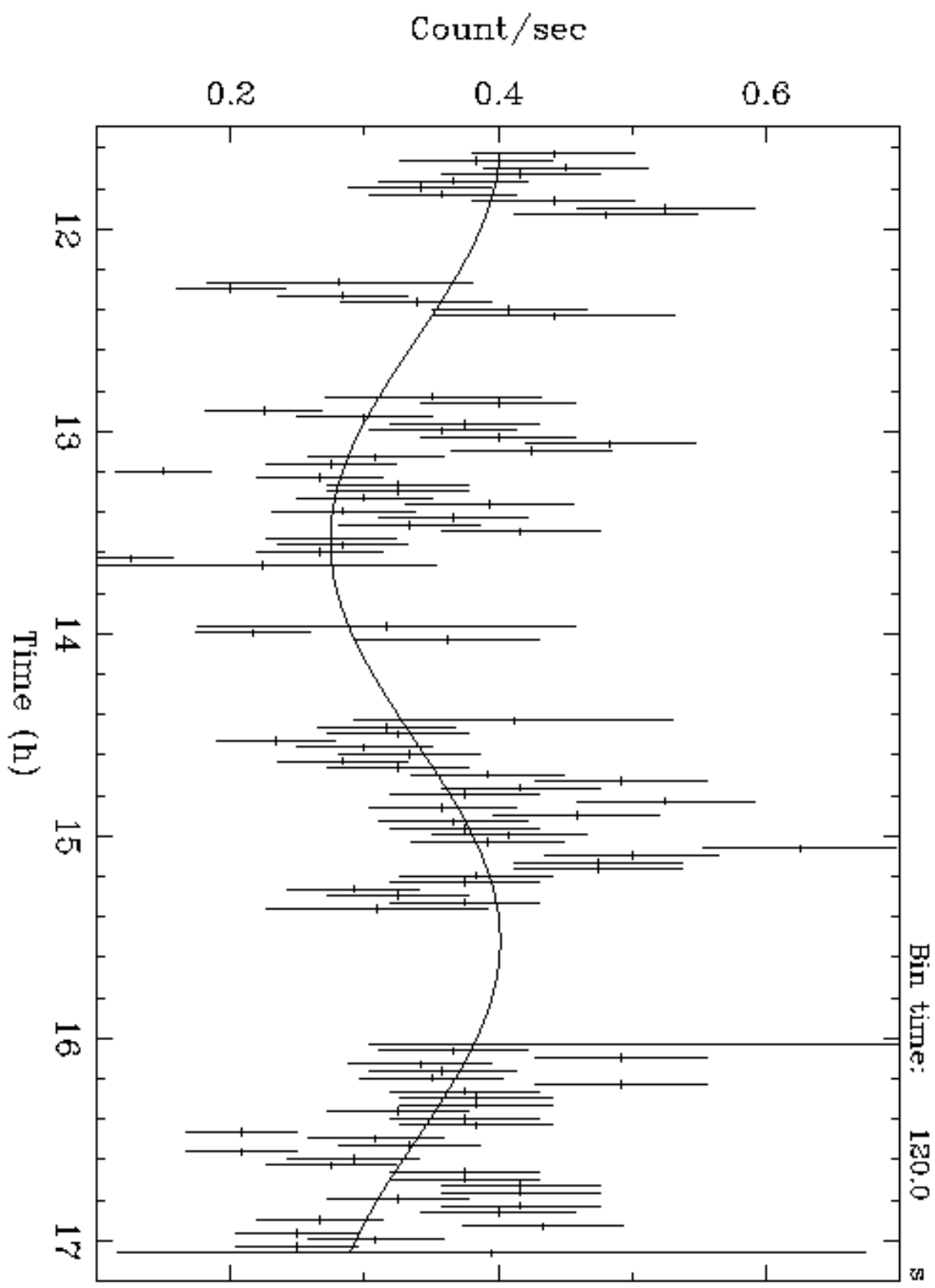








HD 110432



Start Time 10462 11:37:46:665 Stop Time 10462 17: 3:46:665



